

Techno-economic analysis for hydroxy acids production from waste cellulose via alkaline digestion

Farangis Fallahmehneh,^{a*}  Massimiliano Errico,^b Kristian Melin^a and Tuomo Sainio^a



Abstract

BACKGROUND: Alkaline digestion offers a promising route for converting low-grade cellulosic wastes into valuable hydroxy carboxylic acids (HAs). However, the feasibility of producing HAs at process scale, particularly the influence of reactor design on product yields, energy demand, and production costs, remains less explored. This study integrates a detailed kinetic model with process simulation to evaluate techno-economic performance of three process options that differ in reactor configuration and operating temperature.

RESULTS: The batch reactor with a temperature profile (BR-TP) showed the highest selectivity toward glucoisosaccharinic acid (GISA), reaching approximately 65% of total HAs at target temperature of 200 °C, whereas the isothermal batch (BR-IsoT) and isothermal CSTR (CSTR-IsoT) favored smaller hydroxy acids (SHA). The CSTR-IsoT offered shorter residence times at moderate conversions but required dramatically longer times at high conversions; at 200 °C, achieving the target conversion required 38-fold longer time compared with BR-TP. Techno-economic analysis identified BR-TP-200 with the lowest total production cost (TPC) at 0.532 €/kg of product. In contrast, CSTR-IsoT-200 exhibited the highest TPC (0.928 €/kg). Energy consumption varied from 3.93 kW/kg of product in the BR-TP (lowest) to 5.1 kW/kg of product in the CSTR-IsoT. Sensitivity analysis confirmed raw materials as the dominant contributor to cost variability, while utility price fluctuations had minimal effects.

CONCLUSION: Batch operation, particularly BR-TP, delivers the most favorable trade-off between selectivity, energy use, and production cost, confirming the feasibility of alkaline digestion for HAs production. Future studies should validate the model with real wastes and develop improved reactor and alkali-recovery strategies for scale-up.

© 2026 The Author(s). *Journal of Chemical Technology and Biotechnology* published by John Wiley & Sons Ltd on behalf of Society of Chemical Industry (SCI).

Supporting information may be found in the online version of this article.

Keywords: Aspen plus; cellulosic waste valorization; Hydroxy carboxylic acids; kinetic modelling; process design; techno-economic assessment

INTRODUCTION

Cellulosic biomass is commonly defined as renewable or recurrently available organic material, encompassing agricultural crops, forest resources, herbaceous and aquatic plants, lignocellulosic residues, animal-derived waste, municipal solid waste, industrial by-products such as fiber sludge or zero fiber (a cellulose-rich residue with minimal usable fiber content) and other organic waste streams.^{1,2} Limiting the analysis to forest residues, the production of residual biomass obtained from pruning was estimated in 1.34 tons of dry biomass per hectare.³

The increasing accumulation of these wastes opens the necessity to reduce the environmental impact of conventional waste disposal methods and define different valorization routes promoting a circular economy approach by producing sustainable chemicals and products.⁴ Such approaches enhance resource efficiency by ensuring that materials otherwise treated as waste are

converted into useful products instead of being landfilled or incinerated. The valorization of low-grade residues also align with global sustainability targets, including the United Nations Sustainable Development Goals.^{5,6} The move from wastes disposal to valorization is further reinforced by the growing emphasis on techno-economic and sustainability assessments in modern

* Correspondence to: F Fallahmehneh, Lappeenranta-Lahti University of Technology, Department of Separation Science, Mukkulankatu 19, FI-15210 Lahti, Finland. E-mail: farangis.fallahmehneh@lut.fi

^a Lappeenranta-Lahti University of Technology, Department of Separation Science, Lahti, Finland

^b University of Southern Denmark, Department of Green Technology, Odense M, Denmark

biorefinery design, where the valorization of such wastes into value-added chemicals is increasingly recognized as essential for meeting circular-economy targets.⁷

Various physical, chemical, and biological methods have been explored for converting cellulosic wastes into fuels and valuable chemicals. For instance, acid and enzymatic hydrolysis have been widely applied to produce sugars, which serve as precursors for bioethanol, biobutanol, and other fermentation-based chemicals.⁸ Pyrolysis and gasification processes yield bio-oils, syngas, and biochar, which can be refined into hydrocarbons or utilized for energy applications.^{9,10} Advanced chemical transformations have enabled the synthesis of ester compounds, such as alkyl levulinates and alkyl lactates, along with lactones like γ -valerolactone, from cellulose and its derivatives.^{11,12} Additionally, acid-alkali pretreatment methods have demonstrated high efficiency in lignin removal and cellulose recovery, facilitating the production of valuable compounds like sugars, lipids, and bio-oils.^{13,13,14}

However, these methods often face challenges such as the formation of inhibitory by-products for microbial fermentation, high costs and low overall efficiency due to the recalcitrant nature of lignocellulose, the need for long residence times and expensive enzymes or pretreatments that hinder large-scale implementation.¹⁵

Among these approaches, alkaline digestion of waste cellulose has emerged as a promising yet less explored method. This process effectively breaks down the complex structure of cellulose, enhancing cellulose accessibility for further conversion into platform chemicals. One of the most predominant products of alkaline digestion of cellulose include glucoisaccharinic acid (GISA) in its α and β forms, which are of particular interest due to their limited availability from alternative methods. Additionally, smaller hydroxy acids such as 2,5-dihydroxypentanoic acid (2,5-DHPA), 2-hydroxybutanoic acid (2-HBA), lactic acid, glycolic acid, acetic acid, and formic acid can be produced.¹⁶ These compounds find applications in biodegradable polymers and plastics, tissue engineering, cosmetics, and as metal chelating agents.¹⁷⁻¹⁹

Earlier research has focused on studying the kinetics of alkaline degradation of cellulosic materials within two distinct contexts, radioactive waste repositories and pulping processes, emphasizing the preservation of cellulose.^{16,20} Recent studies have identified alkali digestion as a practical and economically viable method for producing hydroxy carboxylic acids (HAs), which are typically difficult and costly to synthesize through conventional chemical pathways. Mattila *et al.*, investigated the effects of temperature, reaction time, and alkali concentration on overall yield and GISA formation during the alkaline degradation of microcrystalline cellulose.²¹ Furthermore, chromatographic techniques have been explored and successfully implemented for the separation and purification of the produced acids.^{22,23}

Most feasibility studies on lignocellulosic biomass fractionation focused on the formation of simple sugars and alcohols.^{24,25} Despite its potential advantages, this conversion route remains understudied, particularly regarding its ability to produce HAs. Furthermore, there appears to be a lack of techno-economic assessments that adequately quantify production costs, energy consumption, and process efficiency, which are essential factors to evaluate the feasibility of industrial-scale implementation. Addressing the mentioned gaps through comprehensive studies is crucial for determining the feasibility and scalability of alkaline digestion as a viable method for converting cellulosic wastes into valuable HAs.

The primary objective of this study is to conduct a techno-economic analysis, assessing production costs and energy

consumption to produce target HAs from alkaline digestion of cellulosic wastes. The targeted HAs include GISA and smaller hydroxy acids being 2,5-dihydroxypentanoic acid (2,5-DHPA), 2-hydroxybutanoic acid (2-HBA), lactic acid, glycolic acid, acetic acid, and formic acid (lumped together and referred to as SHA). To this end, the general scenario of a stand-alone plant utilizing zero-fiber cellulosic feed, water, and sodium hydroxide to produce the mentioned HAs will be investigated. The study evaluates alternative reactor configurations that differ in their temperature and mode of operation. These configurations were selected to represent both batch and continuous processing environments that are relevant for alkaline cellulose digestion. By comparing these different configurations, the study identifies how temperature strategy and reactor type influence overall conversion, product selectivity, and downstream process performance. In addition to the evaluation of production costs and energy consumption, a sensitivity analysis was performed to identify the influence of price fluctuations on the process economics. By addressing these aspects of the process, this study aims to provide valuable insights into the potential of alkaline digestion as a sustainable method for converting low-grade cellulose into high-value platform chemicals. Additionally, it can facilitate further process optimization and integration into upstream and downstream facilities.

METHODS

Process description

The plant is designed to process 7660 kg per hour of a mixture containing 10 wt.% of pure cellulose as biomaterial and 90 wt.% alkaline solution containing 10 wt.% NaOH. The main processing units considered are: feed preheating, alkaline digestion, solid filtration, NaOH recovery, and HAs liberation.

According to the flowsheet of the process plant shown in Fig. 1, the feedstock (FEED-MIX) is preheated in two stages, first in the heat exchanger HX1 using the hot outlet stream of the reactor, then in HX2 using a hot utility to match the overall duty required by the stream. The preheated feed is fed to a jacketed reactor (DIGESTOR) where the cellulose degradation occurs at the desired temperature and at the pressure of 15 bar. The temperature is set by selecting high-pressure steam as a utility for the reactor's jacket. The hot product mixture (PROD-MIX) contains unreacted cellulose and solid components and after pre-heating the feed stream undergoes solid filtration in the filtration unit FILTER operating at 70 °C. Subsequently, the filtrate is sent to the chromatographic column SEP for NaOH recovery. The amount of eluent (WATER) was calculated using data taken from²³ while its temperature is defined to keep the SEP unit to an operative temperature of 50 °C. The diluted recovered base (RE-NAOH) is mixed with a make-up stream to reach the alkaline concentration of 10 wt.% NaOH and recycled to the reactor.

The HA-SALTS stream leaving the SEP unit is treated in 2 ion exchange resin columns operating in sequence. In this way, the Na⁺ ions are removed, and the HA-salts are converted to their acid form.

The regeneration of resins is carried out using 2 M H₂SO₄ as eluent. This step was not included in the simulation, but its influence was considered in the result section using the data published by Heinonen *et al.*²² The final product of the plant is a diluted mixture of HAs that can undergo an evaporation step to obtain a concentrated product stream.

As pure cellulose contains no lignin or hemicellulose, this assumption represents a simplified feedstock compared to real waste biomass. Industrial cellulose-containing wastes typically

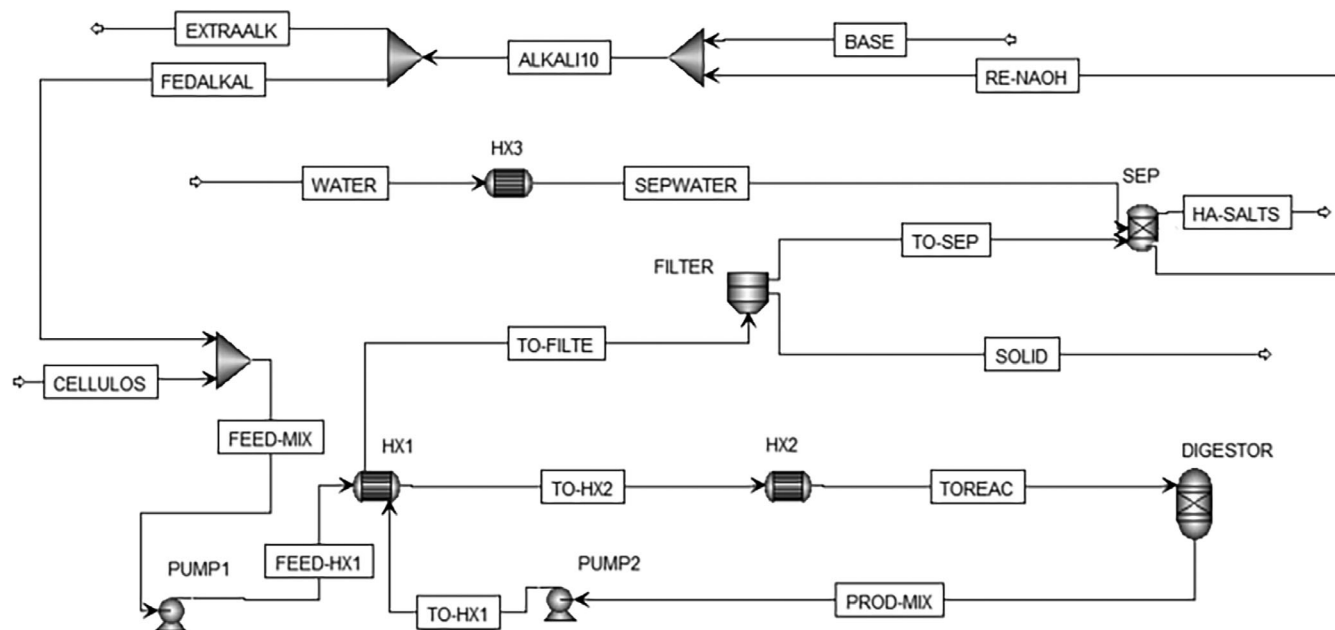


Figure 1. Process flowsheet of hydroxy carboxylic acids (HAs) production from cellulose alkaline digestion.

include these components, which can influence dissolution, alkali consumption, and product distribution. This limitation and its potential impact on process performance are therefore acknowledged. Nonetheless, it should be noted that separation of HAs has been demonstrated even in more complex wastes, such as black liquor containing tens of grams per liter of dissolved lignin. This confirms that the separation scheme applied here remains technically feasible, although performance may differ with real waste-derived feeds.²³ In case of real waste biomass containing lignin and hemicellulose, lignin dissolution increases with cooking time and temperature, and lignin may undergo both depolymerization and repolymerization reactions under alkaline conditions. Hemicelluloses can also degrade into hydroxy carboxylic acids, representing unwanted side reactions observed in alkaline pulping. These behaviors are well documented in pulping literature and help illustrate how real waste biomass differs chemically from pure cellulose, while remaining suitable for alkaline digestion and downstream separation.²⁶

Process design and simulation

The overall process is designed for continuous operation, with three distinct process options differing in the reactor configuration. In the BR-TP configuration, a batch reactor operates with a temperature profile, whereas the BR-IsoT configuration operates the batch reactor isothermally. The CSTR-IsoT option uses an isothermal continuous stirred-tank reactor. In BR-TP and BR-IsoT, the batch reactor operates for 3 h and is integrated into the continuous process using buffer tanks to store the feed and product. A dead time of 1 h was estimated for charging and discharging the reactor.²⁷ The schematic overview of the reactor configurations for the three process options is provided in Fig. 2. In the CSTR-IsoT, the reactor is designed to achieve the same conversion as in BR-IsoT while operating under fully continuous conditions.

Aspen Plus V14 was employed for the process simulation. The cellulose alkaline digestion kinetic model was coded in MATLAB, and it was integrated with Aspen Plus. This was done using Aspen Simulation Workbook (ASW) add-ins of Excel software along with

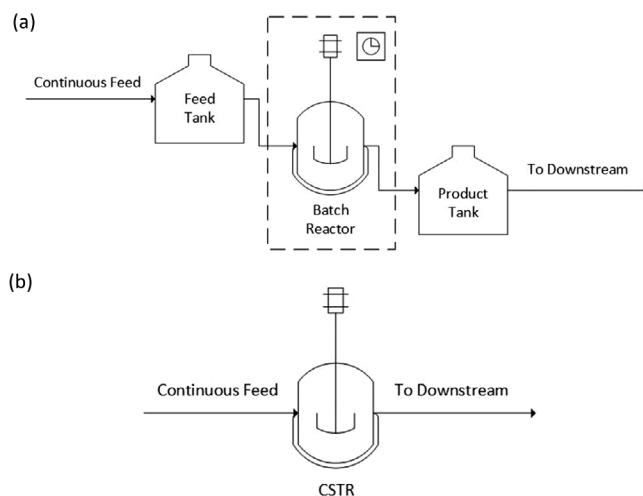


Figure 2. Schematic representation of reactor configurations used in: (a) batch reactor with a temperature profile (BR-TP) and batch reactor isothermal batch (BR-IsoT) and (b) isothermal CSTR (CSTR-IsoT).

a Visual Basic script to predict product yields for the BR-TP, BR-IsoT, and CSTR-IsoT at two temperatures. Figure 3 shows the communication interface between the software.

Sodium hydroxide, water, and sodium salts of the HAs (including sodium glycolate, sodium formate, sodium lactate, sodium acetate, sodium 2-hydroxybutyrate, glutaric acid monosodium salt, and sodium 3-deoxygluconate) were modeled in Aspen Plus as conventional components.

It should be noted that HAs readily convert to their corresponding sodium salts, as the protonated hydrogen is replaced by a sodium ion. Therefore, the sodium salt forms of the HAs were assumed to be present in the product stream. The salt derived from 2,5-DHPA was not available in the Aspen databank. In this case, glutaric acid monosodium salt was selected due to similarities in molecular weight and structure.

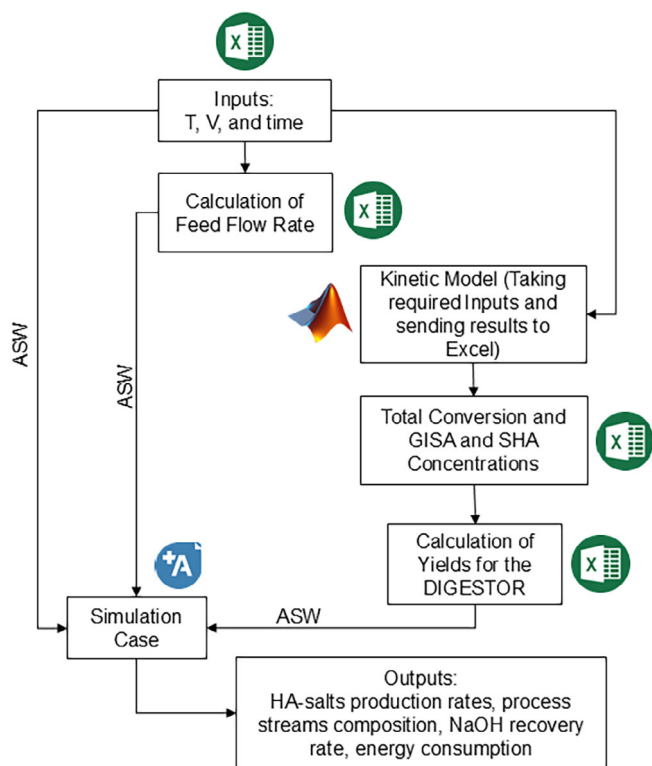


Figure 3. Calculation procedures and interconnections of the calculation environments.

Pure cellulose was treated as a non-conventional component. Its estimated physical properties were validated with the reported data in ChemSrc, 2024 website.²⁸ To achieve mass balance closure, 'Unknown-Products' was added to the simulation as a non-conventional component. This adjustment accounted for the presence of undetectable degradation products associated with the complete conversion of cellulose with 10 wt.% NaOH reported in the experimental work on alkaline cellulose degradation by Laine.²⁹

The NRTL property method was used to estimate the physical properties of the conventional components. Alongside, the JOBACK group contribution method was employed to estimate the missing physical properties. In the case of non-conventional components, the non-conventional general heat capacity (ENTHGEN) and density (DNSTYGEN) models were employed to estimate these properties. The specific enthalpy and density of any nonconventional component are given as the mass-fraction-weighted-average for the enthalpies and densities of its individual constituents.

The reaction kinetic model for cellulose alkaline degradation developed in previous work was utilized for all process options. The kinetic model is grounded in an extensive experimental dataset generated by,²⁹ including detailed measurements of cellulose degradation at different temperatures, NaOH concentrations, and reaction times, ensuring that all kinetic parameters originate from real experimental observations. In this model, cellulose is treated as a material consisting of two structural forms of crystalline and amorphous. The crystalline form first undergoes decrystallization, producing amorphous cellulose that subsequently dissolves into soluble polysaccharides. These dissolved chains degrade through two parallel reactions: (1) peeling,

initiated at the reducing end and yielding GISA and (2) random alkaline hydrolysis, which cleaves internal glycosidic bonds and forms monosaccharides and shorter polysaccharides. Monosaccharides are rapidly converted into SHA, while GISA remains stable under the conditions investigated.

To better reflect the complexity of the kinetic model applied in this work, it should be noted that the reaction network comprises DP + 5 coupled species, where DP is the degree of polymerization of cellulose (DP = 230 in the original model). These species include crystalline cellulose, amorphous cellulose, dissolved polysaccharides of different chain lengths, disaccharides, monosaccharides, GISA, and a lumped pseudo-component representing the smaller hydroxy acids, SHA. Consequently, the system consists of more than 230 simultaneous mass balance equations, each incorporating contributions from decrystallization, dissolution, peeling reactions, random hydrolysis, and temperature-dependent rate expressions. This large and highly interconnected reaction matrix enables the model to capture both macroscopic transformations and detailed molecular-level reactions, forming the basis for the reactor simulations performed in the present study. A detailed description of the rate equations and the values of the kinetic constants were reported in Fallahmehneh & Sainio.³⁰

For BR-TP and BR-IsoT, the batch reactor was modeled assuming constant solution density and volume using the mole balance expressed in Eqn. (1).

$$\frac{dC_j}{dt} = r_j(T), j = 1, \dots, 235 \quad (1)$$

In the BR-TP, a linear temperature profile was applied until the desired target temperature was reached following the experimental heating profile reported by Fallahmehneh & Sainio.³⁰

The behavior of the CSTR-IsoT in terms of product concentrations was described through the steady-state mole balance shown in Eqn. (2).

$$\frac{Q}{V}(C_{j,in} - C_{j,out}) + r_j(T) = 0, j = 1, \dots, 235 \quad (2)$$

In Eqns (1) and (2) Q , V , C , t , r , and T stand for volumetric flow rate, volume of the reactor, molar concentration, time, reaction rate, and temperature, respectively. The subscripts j , in , and out refer to the individual model species, inlet, and outlet stream, respectively.

Techno-economic analysis methodology and financial assumptions

Given the lack of accurate market data for HAs, primarily due to the scarcity of alternative production routes, the cost analysis aims to estimate both the production costs and energy consumption of the process. Additionally, the influence of key operational parameters on overall production costs is assessed.

Aspen Process Economic Analyzer (APEA) was used to perform economic evaluations of the process and estimate the total cost of production. Unlike methods that depend on capacity factors, APEA estimates equipment installation quantities and installed costs directly, making it one of the most robust and versatile tools for cost estimation.

The main components contributing to the capital cost were purchased equipment (in stainless steel, SS 304), piping, civil, instrumentation, electrical, insulation, paint, and contingencies costs. Operational costs were driven by operating labor, maintenance,

supervision, raw materials, and utilities costs. To estimate the operational costs, a plant lifetime of 20 years with continuous 24-h occupancy was assumed. It was also presumed that the plant would operate in three daily shifts for 336 days per year, resulting in a total of 8064 operational hours annually. The accuracy is early-stage techno-economical evaluation of investment cost. The expected accuracy range according to AACE is class 4 corresponding approximately to $\pm 50\%$, which is appropriate for the preliminary nature of this assessment.

The prices utilized for consumables and utilities are shown in Table 1. It is assumed that the waste cellulose is freely available. This is consistent with techno-economic analysis practice for waste-based biorefineries. Many cellulose-containing side streams, such as paper sludge, fines, and water-treatment residues, have no market value and are typically associated with disposal or handling costs.^{31–33} The prices of water and electricity were obtained from reported statistics for Finland in 2024.^{34,35} The price of chemicals were taken from Business Analytiq website.³⁶ The production cost per kilogram of product was defined as shown in Eqn. (3). In this formulation, TPC, TACC, and TOC represent the total production cost, the total annualized capital cost, and the total operational cost, respectively. The TACC was obtained by dividing the total capital cost by the assumed plant's lifetime of 20 years.

$$\text{TPC} = \text{TACC} + \text{TOC} \quad (3)$$

Simulating a continuous process with an integrated batch reactor using buffer tanks approach was not straight forward in an Aspen Plus environment. Therefore, the additional costs of the required tanks and pumps to integrate the batch reactor with the continuous process were calculated using a different method and added to the TPC for processes A and B. These costs were calculated using the factorial method, based on parameters provided by.³⁷ Installation and material correction factors were also considered. Additionally, the costs were actualized with CEPCI 2020 index of 596.2 as well as a fixed currency rate of 0.96 (USD to EUR).

The cost associated with acid liberation step was calculated separately. Also, it was not included in the sensitivity analysis, as it remains the same across all process options due to the consistent HA-salts concentration in the product stream. The cost of the resins required for base recovery (SEP unit) and acid liberation steps was not included in the TPC calculation.

RESULTS AND DISCUSSION

Model results for process options BR-TP, BR-IsoT, and CSTR-IsoT

In case of BR-TP and BR-IsoT, in which the reactors operate in batch mode, the corresponding results presented in Figs 4, 5(a),(c), were

Item	Price
Waste cellulose	0 €/kg
Sodium hydroxide	0.5 €/kg
Water	0.002 €/kg
Sulfuric acid	0.05 €/kg
High pressure steam	2.5 €/GJ
Low pressure steam	1.9 €/GJ
Electricity	0.062 €/kWh

obtained considering a reaction time of 3 h at both investigated temperatures.²⁹ The required reactor volume was calculated using the feed density of 1.15 kg/m³ (estimated by Aspen Plus software) and the fixed feed flow rate described earlier. For CSTR-IsoT, the overall conversion of the isothermal CSTR was fixed to match the overall conversion of the isothermal batch reactor (in BR-IsoT) at each temperature to ensure a fair comparison. The overall conversions for all process options are presented in Table 3. The corresponding reactor volumes required to achieve these conversions in the CSTR-IsoT (43.5 m³ at 180 °C and 750 m³ at 200 °C) are shown in Fig. 6.

Figure 4 shows the product composition of the reactor used (PROD-MIX, Fig. 1) in the BR-TP. With the target temperature of 200 °C, both GISA and SHA concentrations are higher than those obtained at the target temperature of 180 °C, indicating that elevated temperatures accelerate the formation of both GISA and SHA. Importantly, the BR-TP clearly favors GISA formation, with GISA constituting approximately 65% of the total HAs at 200 °C. This behavior reflects the underlying reaction mechanism: gradual heating promotes decrystallization, dissolution of cellulose chains, and peeling reactions in a sequence that supports GISA accumulation. As a result, the temperature-profile batch reactor in the BR-TP is particularly effective in producing GISA alongside SHA. Recent work on thermally assisted alkaline pretreatment has likewise reported that controlled temperature profiles can enhance the accumulation of intermediate products compared with strictly isothermal treatments.^{38,39}

Figure 5(a),(b) present the product compositions (PROD-MIX, Fig. 1) for the reactors used in the BR-IsoT and CSTR-IsoT. The composition is presented against the overall conversion achieved in the reactor to identify the correspondent influence of GISA and SHA.

Both isothermal reactors favor SHA formation over GISA, especially at 200 °C. This is consistent with the reaction pathway; at constant high temperature, dissolved polysaccharides rapidly hydrolyze into monosaccharides, which convert quickly into SHA. As a result, the relative proportion of GISA decreases. In both BR-IsoT and CSTR-IsoT, GISA accounted for less than 55% of total HAs at the temperatures investigated, demonstrating their tendency to favor SHA production more strongly than in BR-TP. These

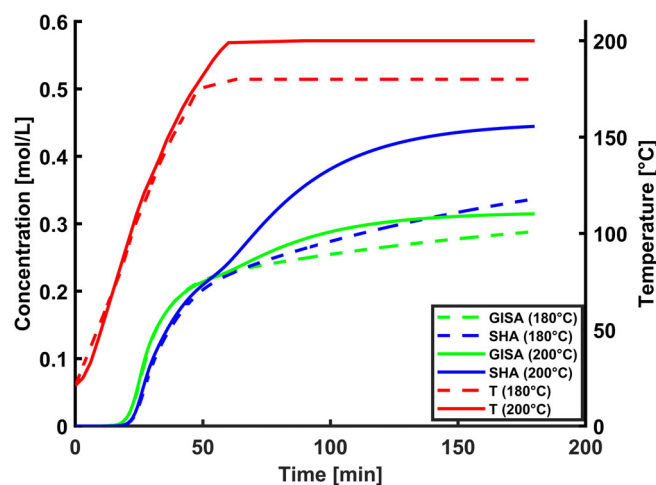


Figure 4. Product composition for the batch reactor with a temperature profile (BR-TP) reactor at two target temperatures: 180°C (dash line) and 200 °C (continuous line).

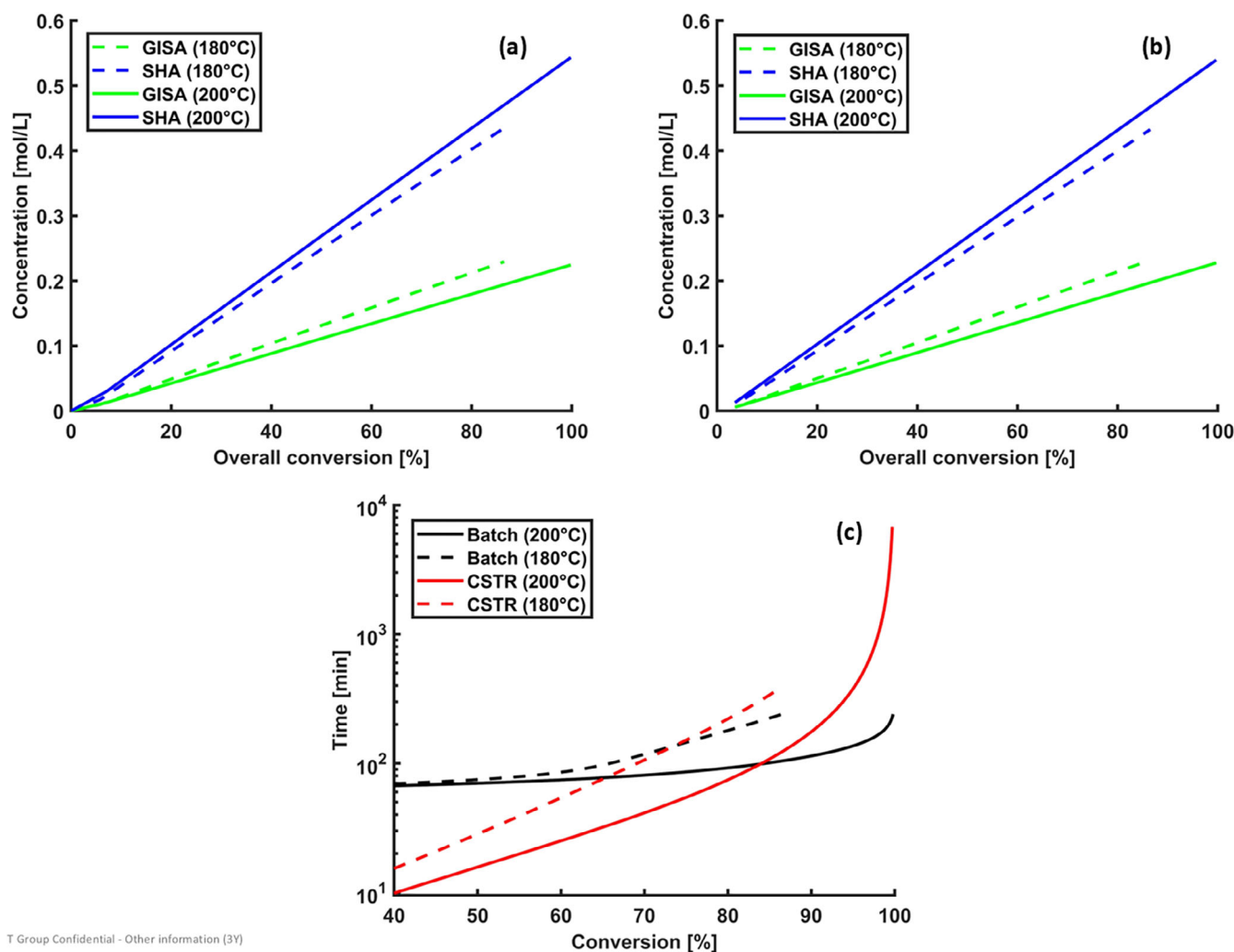


Figure 5. Product composition for the reactors used in the (a) batch reactor isothermal batch (BR-IsoT) and (b) CSTR-IsoT at temperatures of 180 and 200 °C, and (c) required processing time for the batch reactor in BR-IsoT and residence time for the CSTR in CSTR-IsoT as a function of overall conversion at 180 °C and 200 °C.

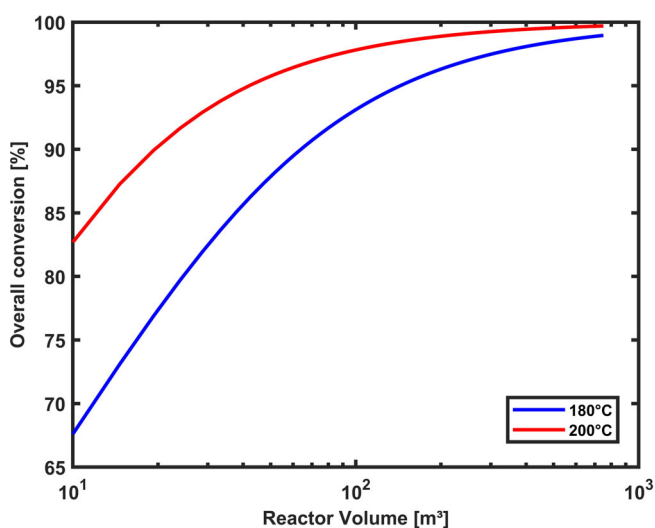


Figure 6. Reactor volume required to reach different overall conversions in the isothermal CSTR (CSTR-IsoT) at 180 °C and 200 °C.

observations align with the rates reported in Table 3. Table 2 summarizes the HA-salt production rates and overall conversions of all process options. While the BR-IsoT and CSTR-IsoT achieve high total HAs yields, the distribution shifts toward SHA. Similar trends in product distribution under different thermal and alkaline treatment conditions have been observed in recent pretreatment studies, where higher severity and isothermal operation favored the formation of smaller degradation products.^{38,39}

Figure 5(c) illustrates the time required to achieve different conversion levels for the isothermal batch reactor and CSTR. The batch reactor's cycle time consists of both the reaction time and a dead time of 1 h per batch, while the CSTR operates continuously without interruptions. At lower conversion levels, the CSTR requires significantly less time than the batch reactor, making it a more time-efficient option. This suggests that when moderate conversions are acceptable, the CSTR offers an operational advantage due to its continuous mode and shorter residence time. However, as conversion increases, the CSTR's required residence time grows sharply, particularly beyond 80% conversion. Quantitatively, the effect is substantial: at 180 °C, the CSTR required nearly twice as long as the batch reactor to reach the target

Table 2. HA-salts production rate and overall conversion of the studied process options at two operating temperatures (180 and 200 °C) and processed feed flowrate of 7660 (kg/h) containing 10 wt.% pure cellulose

Item	BR-TP		BR-IsoT		CSTR-IsoT	
Temperature (°C)	200	180	200	180	200	180
SHA-salts rate (kg/h)	246.617	188.848	299.376	241.445	299.068	241.318
GISA-salt rate (kg/h)	395.964	364.023	286.694	291.646	286.399	291.511
Overall Conversion (%)	99	82	99.8	86.5	99.8	86.5

Table 3. Summary of process data

Item	BR-TP		BR-IsoT		CSTR-IsoT	
Temperature	200	180	200	180	200	180
Produced HA-salts rate (Mton/year)	5.182	4.458	4.726	4.299	4.721	4.297
Total energy consumption (MW)	2.647	2.170	2.600	2.168	2.961	2.211
Energy consumption (kW/kg of HA-salts/h)	4.121	3.926	4.606	4.066	5.057	4.150
Consumed NaOH (Mton/year)	2.972	2.214	2.972	2.214	2.972	2.214

conversion, and at 200 °C, it required approximately 38 times longer. The batch reactor in contrast, maintains a relatively stable cycle time regardless of the conversion target, making it better suited for achieving high conversions efficiently. This highlights an important trade-off: the CSTR is preferable when shorter processing times are desired at moderate conversion, whereas the batch reactor becomes the superior choice when maximizing conversion is the priority.

Overall, the differences observed between BR-TP, BR-IsoT, and CSTR-IsoT arise from the combined effect of their thermal profiles and time characteristics. These operational features ultimately determine the extent to which sequential reactions leading to GISA can proceed relative to the faster pathways that produce SHA. The resulting selectivity trends, higher GISA in the batch reactor with a temperature profile and increased SHA formation under isothermal or continuous operation, are consistent with recent studies on alkaline and hydrothermal cellulose conversion, where shorter times and uniform high-temperature exposure were shown to favor rapid depolymerization and smaller acid products.⁴⁰

Figure 6 shows the relationship between reactor volume and overall conversion in the isothermal CSTR used in CSTR-IsoT. Increasing reactor volume leads to higher overall conversion due to longer residence time, as expected for a CSTR. Temperature strongly influences this behavior: at 200 °C, conversion rises sharply with increasing reactor volume, while at 180 °C, achieving similar conversion requires substantially larger reactor sizes. This observation underscores the importance of carefully balancing reactor volume, residence time, and operating temperature. Comparable techno-economic analyses of continuous biomass conversion processes have identified reactor volume and residence time requirements as key drivers of capital cost and conversion efficiency.^{40,41}

Comprehensive data on stream mass flow rates and operating conditions for all process options can be found in the supplementary information (Tables S1–S3).

Production costs evaluation

This section presents the estimation of HA-salts' production costs derived from waste cellulose *via* alkaline digestion. The techno-

economic analysis includes the evaluation of capital and operational costs for process options BR-TP, BR-IsoT, and CSTR-IsoT.

Table 3 summarizes the key process data, including annual HA-salts production rates and corresponding energy consumption for each process option at 180 and 200 °C. The highest HA-salts production rate is achieved in the BR-TP-200, with approximately 62% GISA in the product mixture, while the lowest rate is observed in the BR-IsoT-180 and CSTR-IsoT-180, at about 4.3 Mton/year. The total energy consumption, including heat and electricity, per kg of HA-salts produced ranges from 3.926 kW/kg in BR-TP-180 to 5.057 kW/kg in CSTR-IsoT-200. The CSTR-IsoT exhibits the highest energy demand, particularly at 200 °C, which correlates with the significantly larger reactor size required to reach similar conversion as BR-IsoT at the same temperature. In contrast, BR-TP and BR-IsoT operate with lower energy consumption, indicating better energy efficiency per unit of product compared to CSTR-IsoT.

The efficiency of NaOH recovery also varies between operating temperatures. At 200 °C, 41.4% of the NaOH fed into the system is recovered, whereas at 180 °C, the recovery increases to 56.3%. Higher temperatures lead to increased reaction rates and consequently greater NaOH consumption, as also reflected in Table 3. This variation has direct implications for operating cost, because NaOH contributes significantly to raw material expenses. Improvements in NaOH recycling or alternative strategies for alkali recovery could therefore provide cost reductions.

Table 4 provides data on jacketed agitated reactor size and cost, which is the major contributor to capital investment in each process option. The required reactor volume increases substantially in the CSTR-IsoT, particularly at 200 °C, where the volume reaches 750 m³, resulting in a dramatic rise in capital cost. In contrast, BR-TP and BR-IsoT require only 20 m³ reactors, leading to significantly lower capital expenditures. The purchased cost of the reactor in the CSTR-IsoT-200 is 7.914 M€, nearly 13 times higher than in the BR-TP and BR-IsoT, where reactor cost ranges from 0.596 to 0.602 M€. These results highlight a critical trade-off: while continuous reactor operation in the CSTR-IsoT may offer operational steadiness, its capital investment is significantly higher, which strongly affects overall feasibility.

This cost difference between batch and continuous configurations reflects a broader trend; under the reaction conditions and kinetics studied here, continuous operation does not provide a cost advantage. The substantial reactor volumes required to achieve high conversions in a CSTR eliminate the typical benefits of continuous processing. In contrast, batch reactors maintain high conversions with much smaller equipment sizes, making them more economically favorable for the scale and chemistry evaluated in this study.

Table 5 presents the total capital and operating costs for each process option, as well as the TPC per kilogram of HA-salts produced. The total capital costs are substantially higher for the CSTR-IsoT, especially at 200 °C, where it reaches 20.705 M€, compared to 7.922 and 7.883 M€ for the BR-TP and BR-IsoT, respectively. The TACC per unit of product is lowest for the BR-TP-200, at 0.076 €/kg, while the CSTR-IsoT-200 exhibits the highest cost, nearly three times greater. The TOC per kilogram of HA-salts ranges from 0.445 €/kg in the BR-TP-180 to 0.709 €/kg in the CSTR-IsoT-200, reinforcing that processes with the batch reactor are more cost-efficient in terms of operational expenses. Regarding the TPC, the lowest is observed in the BR-TP-200 (0.532 €/kg), with only a small increase when operating with lower target temperature. The highest TPC is seen in the CSTR-IsoT-200 (0.928 €/kg). These findings suggest that the BR-TP-200 provides the most cost-effective process option among those evaluated as well as the best balance between capital investment, operational cost, and product yield. It is also worth mentioning that the yield of GISA, as the desired product, in HA-salts mixture is the highest in the BR-TP-180, reaching around 66%.

Taken together, the results highlight clear differences in the economic performance of the three process options and allow a broader interpretation of the underlying cost drivers. The substantially larger reactor volumes required in the CSTR-IsoT led to higher capital costs and greater energy demand, mainly due to the need to maintain uniform temperature and mixing conditions in a much larger vessel. In contrast, the batch reactors used in the BR-TP and BR-IsoT achieve high conversions with

significantly smaller equipment sizes, resulting in lower heating, mixing, and maintenance requirements. These factors collectively explain why, under the reaction conditions and kinetics evaluated in this study, continuous operation does not provide a cost advantage. Instead, the cost savings associated with smaller reactor sizes and reduced utility demands render batch operation more economically favorable.

Overall, the findings demonstrate that the techno-economic viability of HA-salts production is strongly influenced by reactor sizing, raw material consumption, and residence time requirements, with batch configurations offering the best balance between performance and cost at the investigated scale. Recent biorefinery techno-economic studies similarly report that reactor-related capital expenditure, particularly vessel sizing, mixing requirements, and residence-time constraints, often represents one of the largest cost contributors in thermochemical and alkaline biomass conversion processes.^{7,42}

The items considered in the TOC include raw materials, utilities, operating labor, maintenance, and supervision costs. Figure 7 illustrates the contribution of these cost factors to the TOC. Raw material (including sodium hydroxide and water) represents the largest share of TOC, averaging approximately 45% across all process options. This highlights the importance of raw material utilization in determining overall production cost. Similarly, multiple techno-economic studies on lignocellulosic conversion have identified raw materials as the dominant contributors to operating cost, often surpassing utilities by a substantial margin.^{7,43}

Energy consumption, particularly hot utility, accounts for a relatively smaller share, with the highest contribution in process C at 200 °C (11.8% of TOC). This higher utility demand reflects the larger reactor volume and increased heating and mixing requirements to maintain uniform conditions. Labor and supervision costs contribute to a smaller proportion of operational expenses and remain constant across all process options due to identical assumptions regarding the number of shifts and operators. Maintenance costs, however, vary between process options, with the CSTR-IsoT, particularly at 200 °C, incurring the highest maintenance expenses. This is primarily due to the considerably larger reactor size and higher operational demands, which increase wear and tear, leading to greater maintenance requirements and associated costs.

The cost of the acid liberation step is calculated separately and not included in TPC, as it remains constant across all process options due to the identical HA-salt concentrations in the product stream. Therefore, it does not influence sensitivity analysis. The acid liberation step contributes an additional 789.685 K€ to total capital cost and an annual raw material cost of 368.856 K€, which accounts for water and H₂SO₄ consumption.

Table 4. Reactor size and cost data

Process	Reactor size (m ³)	Reactor purchased cost (k€)
BR-TP-180 and BR-IsoT-180	20	596.4
BR-TP-200 and BR-IsoT-200	20	602.2
CSTR-IsoT-180	43.5	930.5
CSTR-IsoT-200	750	7914.2

Table 5. Results of economic evaluation of all process options

Item	BR-TP		BR-IsoT		CSTR-IsoT	
	200	180	200	180	200	180
Temperature						
Total capital cost (M€)	7.9223	7.883	7.9224	7.883	20.705	9.1769
Total purchased equipment (M€)	1.280	1.261	1.280	1.261	9.324	1.628
Total Annualized Capital Cost (€/kg of HA-salts)	0.076	0.088	0.084	0.092	0.219	0.107
Total operating cost (M€/year)	2.359	1.982	2.366	1.983	3.347	2.044
Total operating cost (€/kg of HA-salts)	0.455	0.445	0.501	0.461	0.709	0.476
Total production cost (€/kg of HA-salts)	0.532	0.533	0.585	0.553	0.928	0.583

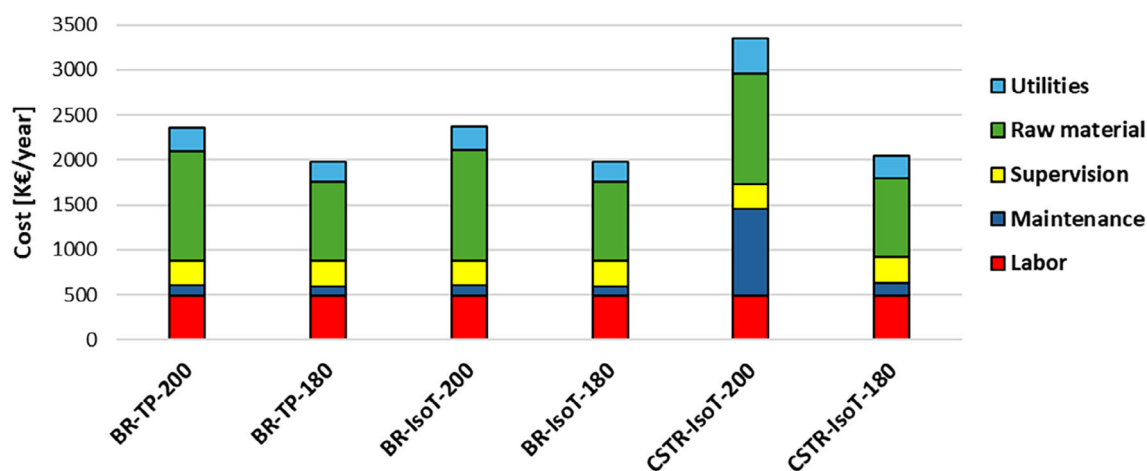


Figure 7. The TOC breakdown for the batch reactor with a temperature profile (BR-TP), BR-IsoT, and CSTR-IsoT at two temperatures.

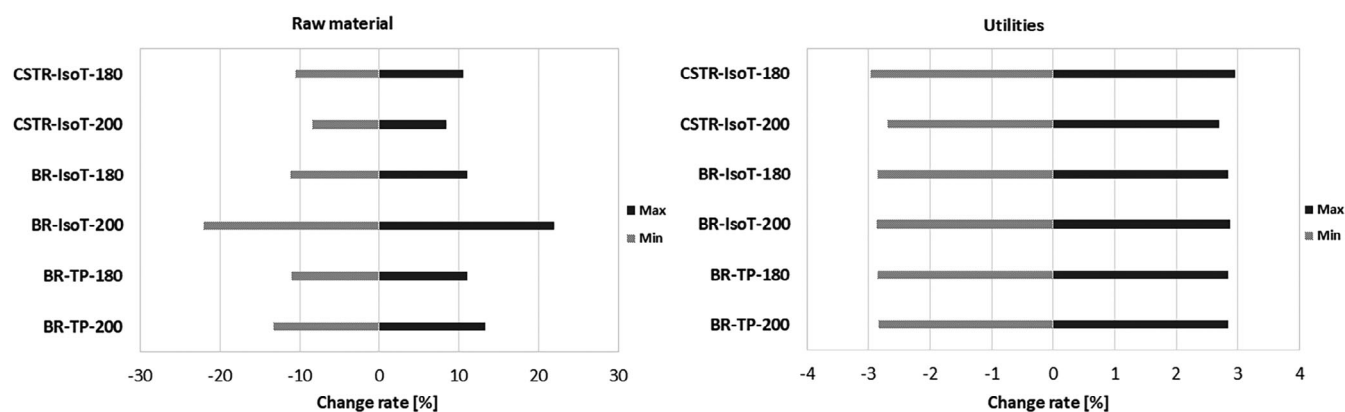


Figure 8. Sensitivity of the TPC to $\pm 30\%$ price changes of raw materials (left) and utilities (right) for the BR-TP, BR-IsoT, and CSTR-IsoT at two temperatures.

Sensitivity analysis

A sensitivity analysis was conducted to evaluate the impact of fluctuations in raw material prices including sodium hydroxide and water and utility prices on TPC of HA-salts. This analysis focuses on external economic factors rather than process-dependent variables such as temperature, which have already been systematically examined in the BR-TP, BR-IsoT, and CSTR-IsoT. Given the significant contribution of the raw materials and utilities to overall process economics, their prices were systematically varied by $\pm 30\%$ to assess how sensitive each process option is to these changes. The results provide insight into the robustness of the process economics and help identify the most influential cost drivers.

For raw material cost fluctuations (Fig. 8 (left)), the analysis reveals notable differences in sensitivity across the studied process options. The BR-IsoT-200 shows the highest sensitivity, with a change rate of 21.97%, indicating that this configuration is particularly vulnerable to increases or decreases in raw material prices. This high sensitivity is largely due to its lower product output compared to the BR-TP, which amplifies the cost impact of raw material variations on a per-kilogram basis. By contrast, the CSTR-IsoT-200 exhibits the lowest sensitivity at 8.36%. The lower sensitivity of this option is due to the fact that its TPC is largely driven by the annualized capital cost, so changes in raw material

prices have a comparatively smaller effect. The remaining process options, BR-TP, BR-IsoT-180, and CSTR-IsoT-180, demonstrate moderate sensitivity, with change rates between 10.52% and 13.26%.

In the case of utilities cost fluctuations (Fig. 8 (right)), the sensitivity patterns differ from those observed for raw materials. All process options exhibit relatively low and closely similar change rates, indicating that utilities costs are considerably less sensitive to price variations. The CSTR-IsoT-180 has the highest change rate at 2.96%, while the same process option at 200 °C presents the lowest at 2.70%. These small variations suggest that utilities-related expenses have only a marginal influence on the TPC, even under substantial ($\pm 30\%$) price changes. Overall, the low sensitivity observed across all process options highlights the relative stability of utility-driven costs and confirms that raw material prices represent the more critical factor shaping the economic robustness of the proposed process configurations.

To assess the influence of cellulosic waste price assumptions on process economics, an additional sensitivity scenario was evaluated by assigning a non-zero cost to the cellulose feed. A value of 50 €/ton was selected as a conservative upper-bound estimate for industrial cellulose-rich residues, reflecting potential handling or transport costs while remaining substantially below the price of market-grade pulps.³³

At the inlet cellulose flow rate of 766 kg/h defined in Section 0, this corresponds to an annual cellulosic feed cost of 308 851 €/year. Including this cost increased the TPC of all process configurations, as expected from the additional raw material expense. The magnitude of the increase varied between 7% to 13%, depending on the reactor configuration and operating temperature. The highest relative increases were observed for the BR-TP-180 and BR-IsoT-180 (both 13%), as these processes originally had the lowest TPC values, making them more sensitive to additional raw-material expenses. Similarly, the BR-TP-200 and BR-IsoT-200 showed increases of approximately 11% to 12%, consistent with their comparatively low baseline TPCs. In contrast, the CSTR-IsoT-200 exhibited the smallest increase (7.1%), because its baseline TPC was already the highest, so the added cellulose cost represents a smaller fraction of the total. The CSTR-IsoT-180 showed a moderate increase (12.2%). However, the relative economic ranking of the process options remained unchanged.

CONCLUSION

In this study, the feasibility of producing hydroxy acids from waste cellulose through alkaline digestion was evaluated by comparing three process options that differ in reactor operating mode and temperature. A detailed process design and simulation framework was developed by integrating a rigorous kinetic model programmed in MATLAB with Aspen Plus. This approach enabled the prediction of product distributions and the assessment of energy consumption and production costs for the three process configurations studied here. Additionally, a sensitivity analysis was conducted to identify the key economic factors that most strongly influence the total production cost.

The results demonstrated that the BR-TP was the most effective configuration for producing GISA, particularly with target temperature of 200 °C, with GISA accounting for approximately 65% of total HAs. In contrast, the Br-IsoT and CSTR-IsoT achieved similar overall HA yields but favored SHA formation, with GISA comprising less than 55% of total HAs at both investigated temperatures. The analysis of cycle times at 180 °C and 200 °C further highlighted operational differences between the isothermal batch reactor and the CSTR used in BR-IsoT and CSTR-IsoT. While the isothermal CSTR offers clear advantages when moderate conversions are acceptable, due to continuous operation and the absence of dead time, it becomes significantly less time-efficient as conversion targets increase. Beyond approximately 80% conversion, the required residence time rises sharply, leading to greatly extended time. For instance, at 180 °C the isothermal CSTR required nearly twice as long to reach the target conversion as the batch reactor, and at 200 °C it required 38 times more time. In contrast, the batch reactor maintained a relatively stable cycle time, making it more suitable for achieving high overall conversions.

The techno-economic assessment showed that the BR-TP-200 provides the most cost-effective configuration among those studied. This process option delivered the highest HA-salts production rate (5.182 Mton/year) while maintaining a relatively low TPC of 0.532 €/kg. In contrast, the CSTR-IsoT exhibited significantly higher capital and operational costs, resulting in a TPC of 0.928 €/kg at 200 °C. Energy consumption varied markedly across process options, ranging from 3.926 kW in the BR-TP-180 to 5.057 kW per unit of product in the CSTR-IsoT-200; this increase is linked to the much larger reactor volume required in continuous operation. NaOH recovery efficiency also declined with increasing temperature, decreasing from 56.3% at 180 °C to

41.4% at 200 °C, illustrating the trade-off between enhanced conversion and higher reagent consumption. The TOC varied across process options studied with the highest TOC of 0.709 €/kg was observed in the CSTR-IsoT-200 and the lowest TOC of 0.445 €/kg in the BR-TP-180. Sensitivity analysis revealed that raw material prices have the strongest influence on TPC, with the BR-IsoT-200 showing the highest sensitivity (21.97%). In contrast, fluctuations in utility prices had a comparatively minor impact, with the highest sensitivity (2.96%) observed for the CSTR-IsoT-180.

Overall, the findings suggest that batch operation, particularly the BR-TP-200, offers the best balance between conversion performance, capital investment, and operating costs. However, further optimization could improve industrial feasibility. Future work could focus on evaluating alternative reactor designs and integration with upstream or downstream processes. Moreover, the experimentally derived kinetics used in this study provide a strong basis for future scale-up studies, where combining the kinetics with hydrodynamic or mass-transfer modeling (e.g., computational fluid dynamics, CFD) could help predict full-scale reactor performance. Additionally, extending the validation to pilot-scale experiments using real waste streams would strengthen confidence in scaling the overall process. Such studies would help assess practical limitations, refine alkali consumption estimates, and verify product distribution under industrially relevant conditions.

ACKNOWLEDGEMENTS

Financial support from Business Finland (5R Refinery project, ID 43303/31/2020) is gratefully acknowledged. Open access publishing facilitated by LUT University, as part of the Wiley - FinELib agreement.

DATA AVAILABILITY STATEMENT

The data supporting the key findings of this study are provided in the Supplementary Materials. Additional data is available from the corresponding author upon request.

CONFLICT OF INTEREST

The authors declare that they have no known competing financial interests or personal relationships that could have appeared to influence the work reported in this paper.

SUPPORTING INFORMATION

Supporting information may be found in the online version of this article.

REFERENCES

- 1 Beckinghausen A, Dahlquist E, Schwede S, Lindroos N, Retkin R, Laatikainen R *et al.*, Downstream Processing of Biorefined Lactate From Lake Bottom Zero Fiber Deposit - a Techno-Economic Study on Energy Efficient Production of Green Chemicals [Internet] (2020). [cited 2025 May 5]. Available from: <https://www.energy-proceedings.org/?p=4179>.
- 2 Ho NWY, Ladisch MR, Sedlak M, Mosier N and Casey E, 3.06 - biofuels from cellulosic feedstocks, in *Comprehensive Biotechnology*, 2nd edn, ed. by Moo-Young M. Academic Press, Burlington, pp. 51–62 (2011) Available from: <https://www.sciencedirect.com/science/article/pii/B97800808885049001550>.
- 3 Velázquez-Martí B, Fernández-González E, López-Cortés I and Salazar-Hernández DM, Quantification of the residual biomass obtained

- from pruning of trees in Mediterranean almond groves. *Renew Energy* **36**:621–626 (2011).
- 4 Madhushree M, Vairavel P, Mahesha G and Bhat KS, A comprehensive review of cellulose and cellulose-based materials: extraction, modification, and sustainable applications. *J Nat Fibers* **21**:2418357 (2024).
 - 5 Blasi A, Verardi A, Lopresto CG, Siciliano S and Sangiorgio P, Lignocellulosic agricultural waste valorization to obtain valuable products: an overview. *Recycling* **8**:61 (2023).
 - 6 UN Office for Sustainable Development [Internet]. 2015 [cited 2025 Apr 8]. Available from: <https://unodsd.un.org/content/sustainable-development-goals-sdgs>
 - 7 Patel R, Rajaraman TS, Rana PH, Ambegaonkar NJ and Patel S, A review on techno-economic analysis of lignocellulosic biorefinery producing biofuels and high-value products. *Results Chem* **13**:102052 (2025).
 - 8 Edwiges T, Roda-Serrat MC, Segovia-Hernández JG, Sánchez-Ramírez E, Tronci S and Errico M, Sustainable bioalcohol production: pretreatment, separation, and control strategies leading to sustainable processes, in *Biofuels and Biorefining*, ed. by Gutiérrez-Antoni C and Gómez Castro FI. Elsevier, Amsterdam, Netherlands, pp. 41–85 (2022) Available from: <https://www.sciencedirect.com/science/article/pii/B9780128241172000041>.
 - 9 Periyasamy S, Karthik V, Senthil Kumar P, Isabel JB, Temesgen T, Hunegnaw BM *et al.*, Chemical, physical and biological methods to convert lignocellulosic waste into value-added products. A review. *Environ Chem Lett* **20**:1129–1152 (2022).
 - 10 Segers B, Nimmegeers P, Spiller M, Tofani G, Jasiukaitytė-Grojzdek E, Dace E *et al.*, Lignocellulosic biomass valorisation: a review of feedstocks, processes and potential value chains and their implications for the decision-making process. *RSC Sustain* **2**:3730–3749 (2024).
 - 11 Takkellapati S, Li T and Gonzalez MA, An overview of biorefinery-derived platform chemicals from a cellulose and hemicellulose biorefinery. *Clean Technol Environ Policy* **20**:1615–1630 (2018).
 - 12 Yao Y, Chen S and Zhang M, Sustainable approaches to selective conversion of cellulose into 5-Hydroxymethylfurfural promoted by heterogeneous acid catalysts: a review. *Front Chem* **10**:880603 (2022) Available from: <https://www.frontiersin.org/journals/chemistry/articles/10.3389/fchem.2022.880603/full>.
 - 13 Alam MM, Greco A, Rajabimashhadi Z and Esposito Corcione C, Efficient and environmentally friendly techniques for extracting lignin from lignocellulose biomass and subsequent uses: a review. *Clean Mater* **13**:100253 (2024).
 - 14 Kululo WW, Habtu NG, Abera MK, Sendekie ZB, Fanta SW and Yemata TA, Advances in various pretreatment strategies of lignocellulosic substrates for the production of bioethanol: a comprehensive review. *Discov Appl Sci* **7**:476 (2025).
 - 15 Mthembu LD, Gupta R and Deenadayalu N, Conversion of Cellulose into Value-Added Products (2021).
 - 16 Knill CJ and Kennedy JF, Degradation of cellulose under alkaline conditions. *Carbohydr Polym* **51**:281–300 (2003).
 - 17 Barralet JE, Tremayne M, Lilley KJ and Gbureck U, Modification of calcium phosphate cement with α -Hydroxy acids and their salts. *Chem Mater* **17**:1313–1319 (2005).
 - 18 Kessler E, Flanagan K, Chia C, Rogers C and Glaser DA, Comparison of alpha- and beta-hydroxy acid chemical peels in the treatment of mild to moderately severe facial acne vulgaris. *Dermatol Surg Off Publ Am Soc Dermatol Surg* **34**:45–50 (2008) discussion 51.
 - 19 Shaw PB, Robinson GF, Rice CR, Humphreys PN and Laws AP, A robust method for the synthesis and isolation of β -gluco-isosaccharinic acid ((2R,4S)-2,4,5-trihydroxy-2-(hydroxymethyl)pentanoic acid) from cellulose and measurement of its aqueous pKa. *Carbohydr Res* **349**:6–11 (2012).
 - 20 Van Loon LR, Glaus MA, Laube A and Stallone S, Degradation of cellulosic materials under the alkaline conditions of a cementitious repository for low- and intermediate-level radioactive waste. II. Degradation kinetics. *J Environ Polym Degrad* **7**:41–51 (1999).
 - 21 Mattila M, Saukkonen L, Laine J, Heinonen J and Sainio T, Conversion of waste cellulose materials into Hydroxy carboxylic acids via alkali digestion. *Waste Biomass Valorization* **16**:5457–5470 (2025). <https://doi.org/10.1007/s12649-025-02990-1>.
 - 22 Heinonen J, Zhao Y and Van der Bruggen B, A process combination of ion exchange and electrodialysis for the recovery and purification of hydroxy acids from secondary sources. *Sep Purif Technol* **240**:116642 (2020).
 - 23 Heinonen J and Sainio T, Novel chromatographic process for the recovery and purification of hydroxy acids from alkaline spent pulping liquors. *Chem Eng Sci* **197**:87–97 (2019).
 - 24 Baral P, Munagala M, Shastri Y, Kumar V and Agrawal D, Cost reduction approaches for fermentable sugar production from sugarcane bagasse and its impact on techno-economics and the environment. *Cellul* **28**:6305–6322 (2021).
 - 25 Matimapa-Kay VG and Laooung-u-thai Y, Biobutanol Feedstock Enhancement: Extract Fermentable Sugar from Sugarcane Bagasse via Alkaline Pretreatment and Steam Hydrolysis In: 2024 the 8th International Conference on Energy and Environmental Science (ICEES 2024) [Internet]. Springer, Cham 2024 [cited 2025 Jan 30]. p. 93–102. Available from: https://link.springer.com.ezproxy.cc.lut.fi/chapter/10.1007/978-3-031-63901-2_7.
 - 26 Gullichsen J, Fogelholm CJ, Arpalahti O, Holmlund K, Hotta A, Huhtinen M *et al.*, Papermaking Science and Technology, Book 6: Chemical Pulping (1999). [cited 2025 Dec 2]; Available from: <https://research.aalto.fi/en/publications/papermaking-science-and-technology-book-6-chemical-pulping/>.
 - 27 Fogler HS, *Essentials of Chemical Reaction Engineering: Essenti Chemica Reactio Engi*. Pearson Education, USA, p. 741 (2010).
 - 28 ChemSrc [Internet] ChemSrc (2024). [cited 2025 Apr 10]. Available from: <https://www.chemsrc.com/en/>.
 - 29 Laine J, Conversion of cellulose and disaccharides to hydroxy carboxylic acids with high temperature alkali treatment [Internet] (2022). [cited 2023 Oct 5]. Available from: <https://lutpub.lut.fi/handle/10024/164567>.
 - 30 Fallahmehneh F and Sainio T, Modelling of reaction kinetics in production of hydroxy carboxylic acids by alkaline degradation of cellulosic waste. *Chem Eng J* **487**:150595 (2024).
 - 31 Mohseni A, Fan L, Gao L, Segal J and Roddick F, A review of carbon recovery in sewage treatment and analysis of product options for a typical water recycling plant. *Environ Sci Water Res Technol* **10**:3090–3121 (2024).
 - 32 Muhammad NIS and Rosentrater KA, Techno-economic evaluation of food waste fermentation for value-added products. *Energies* **13**:436 (2020).
 - 33 Tiller P, Park H, Cruz D, Carrejo E, Johnson DK, Mittal A *et al.*, Techno-economic analysis of biomass value-added processing informed by pilot scale de-ashing of paper sludge feedstock. *Bioresour Technol* **401**:130744 (2024).
 - 34 Statista, Statista (2024). [cited 2025 Apr 3]. Available from: <https://www.statista.com/statistics/1271437/finland-monthly-wholesale-electricity-price/>.
 - 35 Turun Vesihuolto, Turun Vesihuolto (2024). [cited 2025 Apr 3]. Available from: <https://www.turunvesihuolto.fi/en/price-list/>.
 - 36 businessanalytiq, Business Analytiq [cited 2025 Apr 3]. Available from: <https://businessanalytiq.com/>.
 - 37 Towler GP and Sinnott R, *Chemical Engineering Design: Principles, Practice and Economics of Plant and Process Design*. Elsevier/Butterworth-Heinemann, Amsterdam Boston, p. 1245 (2008).
 - 38 Jomnonkhaow U, Imai T and Reungsang A, Microwave-assisted acid and alkali pretreatment of Napier grass for enhanced biohydrogen production and integrated biorefinery potential. *Chem Eng J Adv* **20**:100672 (2024).
 - 39 Saad MBW and Gonçalves AR, Industrial pretreatment of lignocellulosic biomass: a review of the early and recent efforts to scale-up pretreatment systems and the current challenges. *Biomass Bioenergy* **190**:107426 (2024).
 - 40 Islam MT, Saha N, Klinger JL and Reza MT, Technoeconomic assessment comparison of batch and continuous hydrothermal carbonization of waste corn stover into advanced biorefinery feedstock. *Biofuels Bioprod Biorefin* **17**:1668–1680 (2023).
 - 41 Pandit K, Kudva IK, Shinde SG, Boose C and Fan LS, Techno-economic assessment of biomass-to-liquid fuel production via chemical looping in comparison to conventional pathways. *Fuel Process Technol* **278**:108341 (2025).
 - 42 Pérez-Almada D, Galán-Martín Á, Mar Contreras M del and Castro E, Integrated techno-economic and environmental assessment of biorefineries: review and future research directions. *Sustain Energy Fuels* **7**:4031–4050 (2023).
 - 43 Onu Olughu O, Tabil LG, Dumonceaux T, Mupondwa E, Cree D and Li X, Technoeconomic analysis of a fungal pretreatment-based cellulosic ethanol production. *Results Eng* **19**:101259 (2023).